

Effect of Zr-Ti substitution on microstructure of the Fe-Zr/Ti-Cu-B nanocrystalline alloy

M. Miglierini^{1,2}, R. Vittek¹, P. Švec³, D. Janičkovič³

¹*Slovak University of Technology, Ilkovičova 3, 812 19 Bratislava, Slovak Republic*

²*Center for Nanomaterials Research, Palacky University, Svobody 26, 771 46 Olomouc, Czech Republic*

³*Institute of Physics, Slovak Academy of Sciences, Dúbravská cesta 9, 845 11 Bratislava, Slovak Republic*

Received 9 January 2009, received in revised form 10 February 2009, accepted 16 February 2009

Abstract

Fe₈₀Zr₇Cu₁B₁₂ alloy belongs to the NANOPERM-type family of nanocrystalline alloys. In this work, we concentrate on the study of mutual relation between microstructure, hyperfine magnetic fields and substitution of Zr by Ti using Mössbauer spectrometry, X-ray diffraction and transmission electron microscopy. A complete substitution of Zr by Ti in the amorphous alloy has led to a decrease of the mean hyperfine field by almost 1 T. Nevertheless, a partial substitution, i.e. Zr₄Ti₃ has no appreciable effect on the magnetic behaviour. After extensive annealing, this alloy shows the lattice parameter of 2.866 Å that indicates almost pure bcc-Fe phase. Such perfect arrangement of the nanocrystallites is, however, not observed in the Zr₇- and Ti₇-containing nanocrystalline alloys.

Key words: hyperfine interactions, NANOPERM, Mössbauer spectrometry, nanocrystalline alloys

1. Introduction

Higher value of saturation magnetization and permeability as compared to those of conventional FeNb-SiBCu alloys were obtained for a new class of iron based nanocrystalline FeMB(Cu) alloys, where M is a metal such as Zr, Nb, Ta, Mo, Ti [1, 2]. Excellent soft magnetic properties designate these nanocrystalline alloys as good candidates for practical applications [3, 4]. These alloys contain crystalline grains of 7–20 nm in size, which are situated into amorphous matrix. This special type of structure is obtained by controlled annealing of an amorphous precursor thus forming a two-phase system [5]. To understand the origin of these materials it is necessary to concentrate on their microstructure [6]. A variety of sophisticated analytical tools including tracer diffusion studies [7, 8] are employed for this purpose. Especially useful seems to be Mössbauer spectrometry, which can assess separate contributions from disordered (amorphous) as well as ordered (nanocrystalline) phases [9].

Microstructure and magnetic after-effects were

recently investigated for the Fe₈₀Zr₄Ti₃Cu₁B₁₂ alloy [10]. In addition, other concentrations were also studied for nanocrystalline Fe₈₂(Zr₄Nb₃)Cu₁B₁₀ and Fe₈₀(Zr₄Mn₃)Cu₁B₁₂ alloys [11]. In these studies, Mössbauer spectrometry was used as the principal method of characterization. In the current work, we concentrate on mutual relation between microstructure and hyperfine interactions in the Fe₈₀Zr₇Cu₁B₁₂ NANOPERM-type alloy after a substitution of Zr by Ti. Along with Mössbauer spectrometry also X-ray diffraction and transmission electron microscopy is used.

2. Experimental details

Amorphous precursors of Fe₈₀Zr₇Cu₁B₁₂, Fe₈₀Zr₄Ti₃Cu₁B₁₂ and Fe₈₀Ti₇Cu₁B₁₂ alloys were prepared by rapid quenching on rotating wheel in a protective Ar atmosphere. They were produced in a form of ribbons about 20 μm thick and 2–8 mm wide. Nanocrystalline samples were prepared by isothermal 1 hour

*Corresponding author: tel.: +421 2 602 91 167; fax: +421 2 654 27 207; e-mail address: marcel.miglierini@stuba.sk

annealing of the as-quenched alloys in a vacuum. The temperatures of annealing were chosen according to the results of DSC so that the first crystallization step was covered.

^{57}Fe Mössbauer spectroscopy was performed by a conventional constant acceleration apparatus with a $^{57}\text{Co}(\text{Rh})$ source. The absorbers were composed of several 1.2 cm long ribbons of the investigated alloys so that the total sample area was 1 cm^2 . They were measured at room temperature (300 K). Mössbauer spectral parameters were refined by the Confit fitting software [12]. The fitting procedure used is described in more details below.

The microstructure of as-quenched and nanocrystalline samples was analysed by X-ray diffraction (XRD) with $\text{Cu K}\alpha$ radiation in Bragg-Brentano configuration with graphite monochromator in the diffracted beam and by transmission electron microscopy (TEM) using JEOL 2000FX at 200 kV. Samples for TEM were polished by Ar ion beam milling in Gatan PIPS; samples were prepared in conventional way from as-quenched or thermally treated disks by ion beam polishing.

Detailed quantitative analysis of X-ray diffraction patterns by the Scherrer method and by Rietveld refinement using Bruker TOPAS software was used to determine the lattice parameters, crystalline phase volume content and grain size. The accuracy of determination of these parameters was better than 0.0004 \AA , 5 % and 2 nm, respectively.

3. Results and discussion

3.1. Mössbauer spectrometry

We have annealed the as-quenched samples for one hour in a broad temperature range extended over the first crystallization peak as determined from DSC measurements. Subsequently, room temperature Mössbauer spectra were recorded. Depending upon the temperature of annealing, structural relaxation of the amorphous precursors and eventually partial crystallization was observed. Mössbauer spectra of the structurally relaxed samples show smeared shapes typical for amorphous alloy in magnetically ordered state with well-developed asymmetry. The latter indicates a presence of structural regions with different hyperfine interactions. Consequently, these spectra were fitted by three distributions of magnetic fields.

The Mössbauer spectra of partially crystallized samples were fitted using the procedure described elsewhere [13]. An example of this fitting model is shown in Fig. 1 for the $\text{Fe}_{80}\text{Zr}_4\text{Ti}_3\text{Cu}_1\text{B}_{12}$ alloy annealed for 1 hour at 525°C .

Some selected examples of transmission room temperature Mössbauer spectra of $\text{Fe}_{80}\text{Zr}_7\text{Cu}_1\text{B}_{12}$,

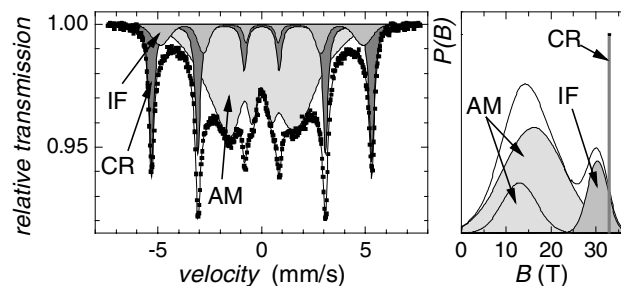


Fig. 1. Fitting model applied to the Mössbauer spectra of nanocrystalline samples: amorphous (AM), crystalline (CR), and interfacial regions are distinguished. Corresponding distributions of hyperfine fields are also shown. A room temperature Mössbauer spectrum of the $\text{Fe}_{80}\text{Zr}_4\text{Ti}_3\text{Cu}_1\text{B}_{12}$ alloy annealed for 1 hour at 525°C is shown.

$\text{Fe}_{80}\text{Zr}_7\text{Ti}_3\text{Cu}_1\text{B}_{12}$ and $\text{Fe}_{80}\text{Ti}_7\text{Cu}_1\text{B}_{12}$ alloys annealed for 1 hour at the indicated temperatures are shown in Fig. 2. In general, two types of spectral shapes are observed: (i) broad and overlapped lines similar to those found in the as-quenched alloys which indicate an amorphous nature of the structure, and (ii) well distinguished narrow sextets with widened tails towards small velocities both being superimposed upon broad features located in the central part of a spectrum. The narrow lines represent crystalline phase (CR) formed during the annealing whereas the central broad line is assigned to the residual amorphous matrix (AM). The remaining third component belongs to the so-called interface regions (IF) which consist of the atoms located at the surface of nanocrystalline grains as well as those Fe atoms that belong to the AM phase but are in close contact with nanograins [13].

At low enough annealing temperatures, Mössbauer spectra of the Zr- and ZrTi-containing alloys exhibit broadened six-line patterns which correspond to amorphous structure with weak ferromagnetic ordering. The onset of crystallization occurs in these alloys above 450°C . It is demonstrated by well developed narrow CR lines. In the Ti-containing alloy, CR phase appears already after the annealing at 420°C . The differences in the kinetics of crystallization are clearly seen and they are caused by variations in the composition of the as-quenched precursor. A gradual increase in intensity of narrow lines is observed in all compositions with rising temperature of annealing.

Results of quantitative evaluation of the Mössbauer spectra of annealed $\text{Fe}_{80}\text{Zr}_7\text{Cu}_1\text{B}_{12}$, $\text{Fe}_{80}\text{Zr}_4\text{Ti}_3\text{Cu}_1\text{B}_{12}$ and $\text{Fe}_{80}\text{Ti}_7\text{Cu}_1\text{B}_{12}$ alloys are presented in Figs. 3, 4 and 5, respectively. Dependences of average hyperfine magnetic fields B_f and relative fractions A_f ($f = \text{AM}, \text{CR}$ and IF) upon the temperature of annealing T_a are provided as derived from the corresponding Mössbauer spectra.

According to the B_{CR} values, the crystalline phase

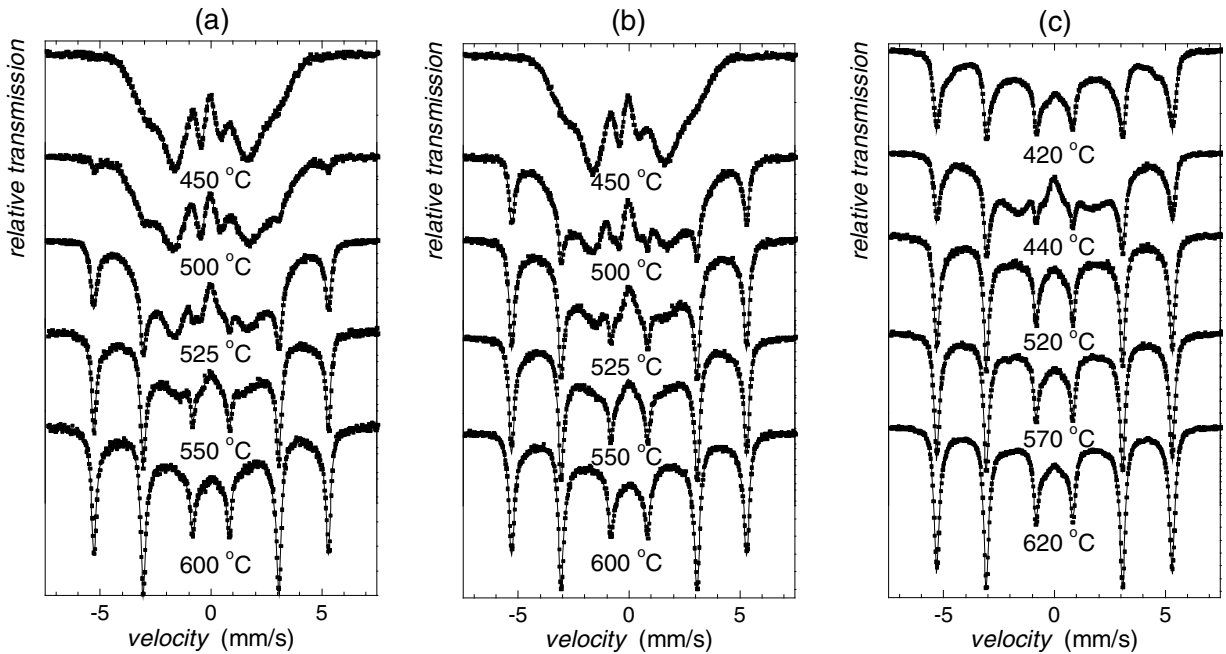


Fig. 2. Mössbauer spectra of $\text{Fe}_{80}\text{Zr}_7\text{Cu}_1\text{B}_{12}$ (a), $\text{Fe}_{80}\text{Zr}_4\text{Ti}_3\text{Cu}_1\text{B}_{12}$ (b) and $\text{Fe}_{80}\text{Ti}_7\text{Cu}_1\text{B}_{12}$ (c) alloys taken at room temperature after one-hour annealing at the indicated temperature.

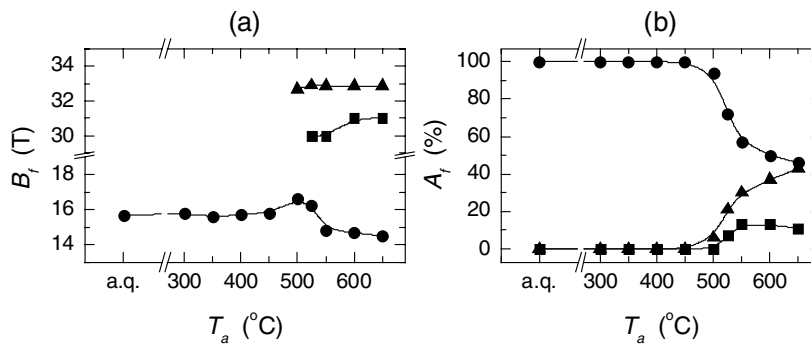


Fig. 3. Average hyperfine field B_f (a) and relative fraction A_f (b) plotted against the temperature of annealing T_a for the $\text{Fe}_{80}\text{Zr}_7\text{Cu}_1\text{B}_{12}$ alloy: $f = \text{CR}$ (triangles), IF (squares) and AM (circles).

formed is bcc-Fe. It is noteworthy, that hyperfine fields of the IF regions are about 2–3 T lower than those of the CR phase. The difference of 3 T is observed for rather small amounts of CR nanograins as in the $\text{Fe}_{80}\text{Zr}_7\text{Cu}_1\text{B}_{12}$ alloy annealed at about 500 °C. From the chemical point of view, CR and IF components are similar one to another as it is confirmed also by close-to-zero isomer shift values ($\text{IS} \sim 0.02 \text{ mm s}^{-1}$). Nevertheless, structural alternations between these two types of resonant Fe atoms are demonstrated via their hyperfine field values. Symmetry breaking of the IF atoms is responsible for the observed decrease in B_{IF} . On the other hand, practically no change in B_{CR} values with the temperature of annealing confirms that these phases are well defined over the first step of crystallization.

As far as the amorphous residual phase is con-

cerned, it demonstrates moderate (overall) decrease in B_{AM} values for Zr- and Zr/Ti-containing alloys. In the early stages of annealing, i.e. below the onset of crystallization, the decrease in B_{AM} is caused by structural rearrangement of the atoms due to structural relaxation. Moderate heating leads to changes of quenched-in structural positions of the resonant atoms aiming to acquire energetically more favourable positions. This effect is more pronounced for the Zr/Ti alloy. The Ti-containing alloy was annealed at rather high temperatures when the crystallization has already started so that we do not see changes in completely amorphous sample.

An interesting feature in the B_{AM} dependences appears at the onset of crystallization when a sudden increase in B_{AM} is seen in Figs. 3a, 4a and 5a for all alloys. This is most probably due to changes in com-

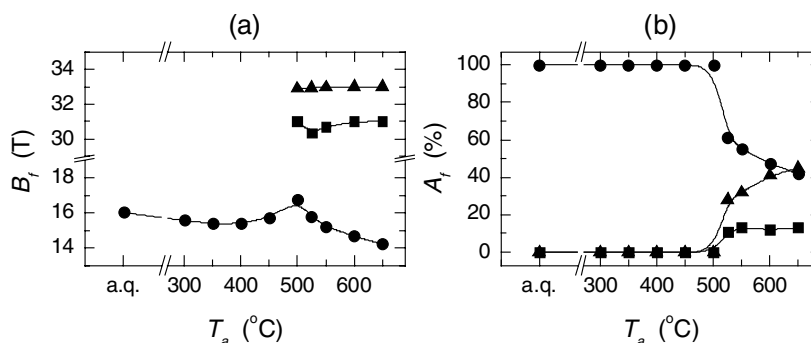


Fig. 4. Average hyperfine field B_f (a) and relative fraction A_f (b) plotted against the temperature of annealing T_a for the $\text{Fe}_{80}\text{Zr}_4\text{Ti}_3\text{Cu}_1\text{B}_{12}$ alloy: $f = \text{CR}$ (triangles), IF (squares) and AM (circles).

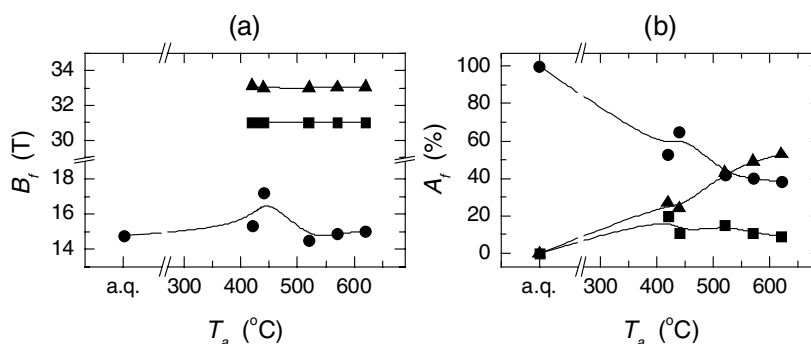


Fig. 5. Average hyperfine field B_f (a) and relative fraction A_f (b) plotted against the temperature of annealing T_a for the $\text{Fe}_8\text{Ti}_7\text{Cu}_1\text{B}_{12}$ alloy: $f = \text{CR}$ (triangles), IF (squares) and AM (circles).

position of the residual amorphous phase when the latter is depleted to Fe, which forms the nanocrystallites. Thus, the effective concentration of the compositional elements is changed and this is demonstrated in the associated B_{AM} -values. Toward higher temperatures of annealing (i.e., higher degree of crystallization) the changes in chemical and/or topological short-range order cause again a decrease of hyperfine fields in the residual amorphous matrix.

Figures 3b, 4b and 5b introduce the evolution of relative contributions of the spectral components, which represent individual structural phases with temperature of annealing. After the onset of crystallization a gradual increase of the CR phase (solid triangles) is observed. After partial substitution of Zr by Ti, more rapid increase in A_{CR} is seen. The crystallization temperature was determined from the Mössbauer effect experiments to be of about 490°C, 480°C and well below 420°C for the $\text{Fe}_{80}\text{Zr}_7\text{Cu}_1\text{B}_{12}$, $\text{Fe}_{80}\text{Zr}_7\text{Ti}_3\text{Cu}_1\text{B}_{12}$ and $\text{Fe}_{80}\text{Ti}_7\text{Cu}_1\text{B}_{12}$ alloys, respectively. Together with CR also the IF phase appears. Its content is stabilized and shows a decrease towards high temperatures of annealing because of enhanced contribution of the nanograins, which start to agglomerate. Consequently, contribution from their surface atoms is reduced.

Comparing different compositions we can state that the most rapid crystallization is found in the

Ti-containing alloy in which a 50 : 50 ratio of the AM and CR components is reached after annealing at about 520°C. Detectable differences in the crystallization kinetics are observed between Zr- and Zr/Ti-containing alloys even though from the point of view of their magnetic behaviour they seem to be very alike as discussed at the beginning of this section. Thus, a conclusion can be proposed that Ti accelerates the progress of crystallization in the $\text{Fe}_{80}(\text{Zr},\text{Ti})_7\text{Cu}_1\text{B}_{12}$ NANOPERM-type alloy.

3.2. X-ray diffraction and TEM

XRD performed upon as-quenched Fe-Zr/Ti-Cu-B alloys unveiled a presence of quenched-in bcc-Fe phase with a pronounced texture. This is demonstrated by (200) reflections at $\sim 65^\circ$ in Fig. 6 (a.q.). For the Zr7- and Zr4Ti3-samples, the size of crystallites is less than 4 nm whereas for the Ti7-alloy the nanocrystals are of about 8 nm.

After annealing, an evolution of bcc-Fe reflections superimposed upon broad lines, which are ascribed to the residual amorphous phase, is observed in the XRD patterns. Using both the Scherrer formula and Rietveld refinement, quantitative features that characterize the crystalline phase in terms of its relative contents, lattice parameter as well as grain size were

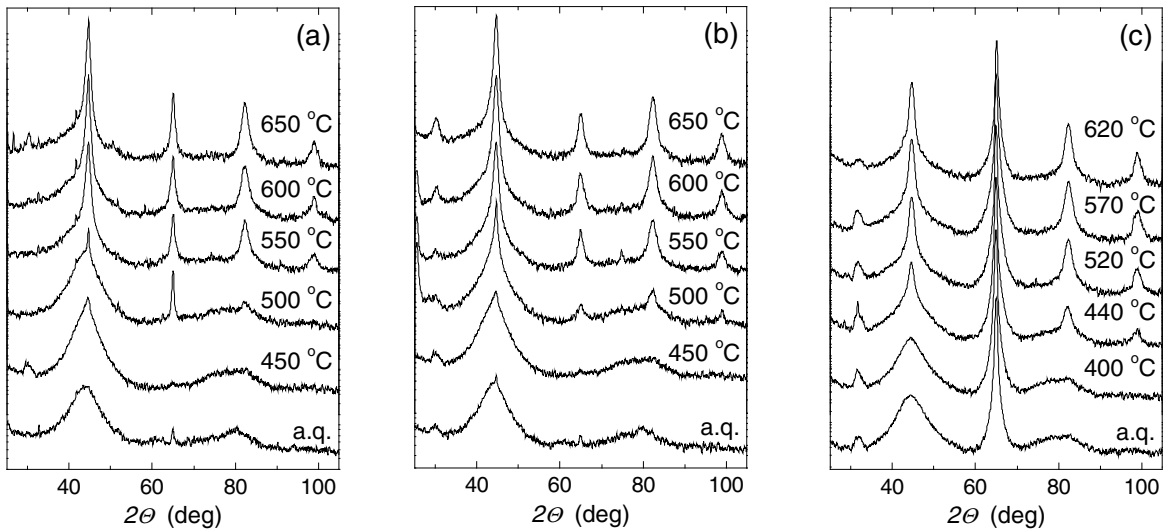


Fig. 6. XRD of the $\text{Fe}_{80}\text{Zr}_7\text{Cu}_1\text{B}_{12}$ (a), $\text{Fe}_{80}\text{Zr}_4\text{Ti}_3\text{Cu}_1\text{B}_{12}$ (b), and $\text{Fe}_{80}\text{Ti}_7\text{Cu}_1\text{B}_{12}$ (c) alloys annealed at the indicated temperatures (a.q. – as-quenched).

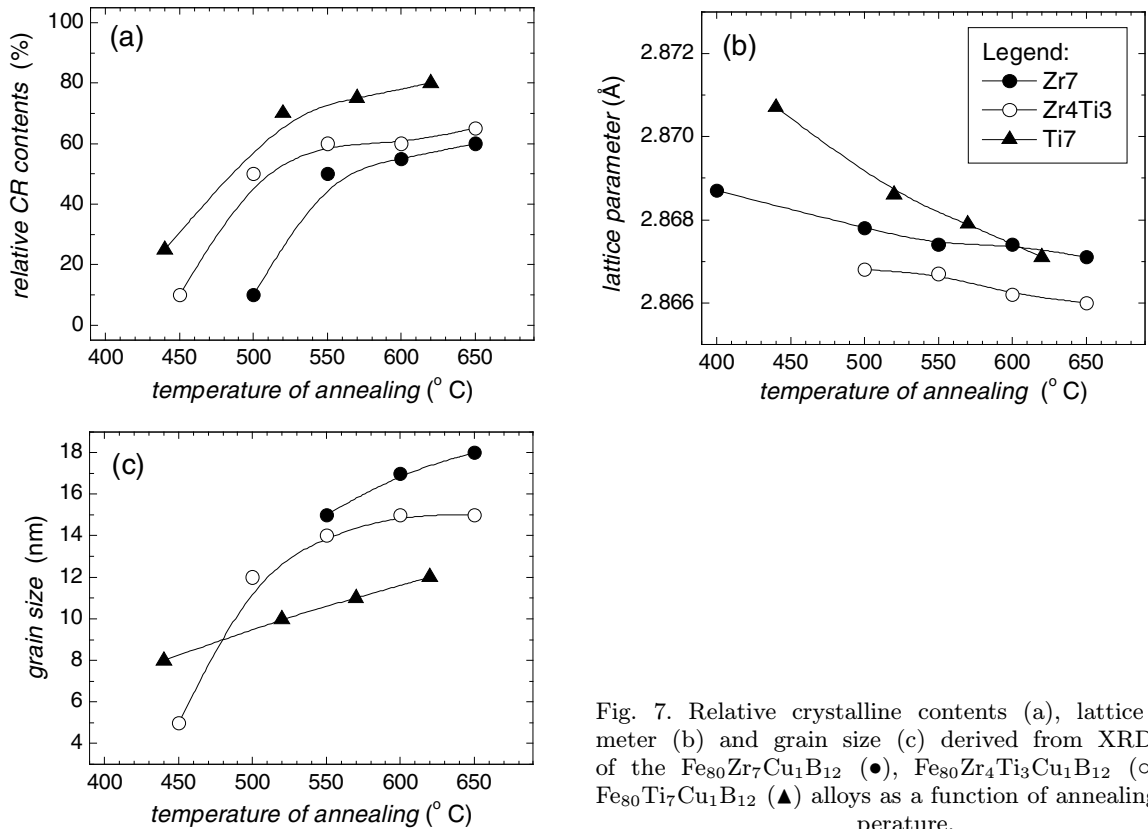


Fig. 7. Relative crystalline contents (a), lattice parameter (b) and grain size (c) derived from XRD data of the $\text{Fe}_{80}\text{Zr}_7\text{Cu}_1\text{B}_{12}$ (●), $\text{Fe}_{80}\text{Zr}_4\text{Ti}_3\text{Cu}_1\text{B}_{12}$ (○) and $\text{Fe}_{80}\text{Ti}_7\text{Cu}_1\text{B}_{12}$ (▲) alloys as a function of annealing temperature.

evaluated. They are plotted in Fig. 7 as a function of annealing temperature. In order to avoid the effect of as-quenched textured crystallinity the angular region around the (200) reflection was excluded from the analyses.

The relative contents of the crystalline phase agree reasonably well with the Mössbauer effect data if the relative contributions of the CR and IF spectral components are added together. The lattice parameter

decreases with the temperature of annealing, i.e. an increased amount of the crystalline phase and tends to approach the value of 2.866 Å characteristic for pure bcc-Fe. It is noteworthy that the well-annealed Zr4Ti3-sample almost reaches this value. Both Zr7- and Ti7-alloys have somewhat higher lattice parameter, which indicates possible deviations in perfect arrangements of atoms in the bcc crystalline lattice. The lower is the annealing temperature the higher mis-

match in the lattice parameters is observed for these two particular compositions of the nanocrystalline alloys.

The size of nanocrystalline bcc-Fe grains in Fig. 7c, which are formed at high temperatures of annealing, monotonously increases with respect to the composition of the alloy (Ti → ZrTi → Zr).

Small diffraction peak in low-angle region (at ~ 30 – 35 deg) is present in nearly all diffraction patterns but does not show a systematic evolution with annealing (or crystallinity content). This feature is present also in all electron diffraction patterns in Fig. 8, suggesting that if its origin is in the presence of oxides of Zr and Ti, these oxides might be present in tiny amounts throughout the entire sample volume. The positions of these rather broad peaks allow assuming that they correspond to orthorhombic ZrO_2 or ZrTiO_4 and rhombohedral Ti_2O_3 in samples with 0, 3 and 7 at.% of Ti, respectively. The presence of these anomalies also in as-quenched samples indicates that they probably originate from oxide traces (impurities), which were present in the Zr and Ti metals used for preparation of the master alloys and which were quenched-in into the ribbon samples. They differ in structure (and size) from the monoclinic and tetragonal Zr-oxides, the formation of which has been observed during nanocrystallization in oxygen-containing atmospheres [14]. A more accurate assessment of the presence and type of these phases is not possible by the methods used due to their marginal volume content and also their small size; even high-magnification TEM analysis was unable to distinguish the presence of particles other than bcc-Fe.

Examples of bright-field TEM images acquired from the annealed nanocrystalline alloys are illustrated in Fig. 9. Excellent agreement between the grain sizes of bcc-Fe obtained from XRD and TEM analyses suggests that (excepting a thin surface layer quenched-in crystallinity) the iron nanograins are in all cases oriented randomly with respect to each other and without observable mutual coherence [15, 16]. Even a certain small degree of agglomeration of nanograins observed in dark-field images of $\text{Fe}_{80}\text{Ti}_7\text{Cu}_1\text{B}_{12}$ sample (not shown) does not increase the coherence. This and the overall homogeneity of distribution of nanograins in the matrix suggest that the nucleation from amorphous phase is truly random and that the formation of interfacial layer during nanocrystallization is not significantly hindered by grain impingement.

4. Conclusions

We investigated mutual relation between microstructure, hyperfine magnetic fields and substitution of Zr by Ti in the $\text{Fe}_{80}(\text{Zr},\text{Ti})_7\text{Cu}_1\text{B}_{12}$ NANOPERM-

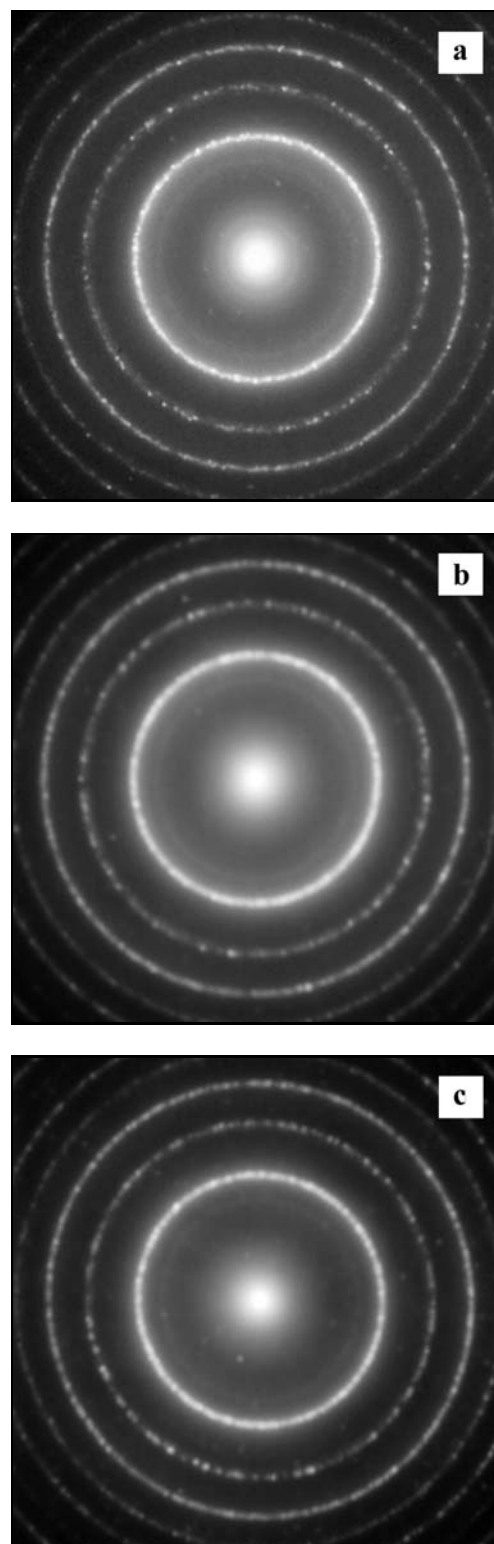


Fig. 8. Electron diffraction patterns of the $\text{Fe}_{80}\text{Zr}_7\text{Cu}_1\text{B}_{12}$ (a), $\text{Fe}_{80}\text{Zr}_4\text{Ti}_3\text{Cu}_1\text{B}_{12}$ (b) and $\text{Fe}_{80}\text{Ti}_7\text{Cu}_1\text{B}_{12}$ (c) alloys annealed at 650°C , 650°C and 620°C , resp.

-type alloy. A complete substitution has caused that the average hyperfine magnetic field of the as-

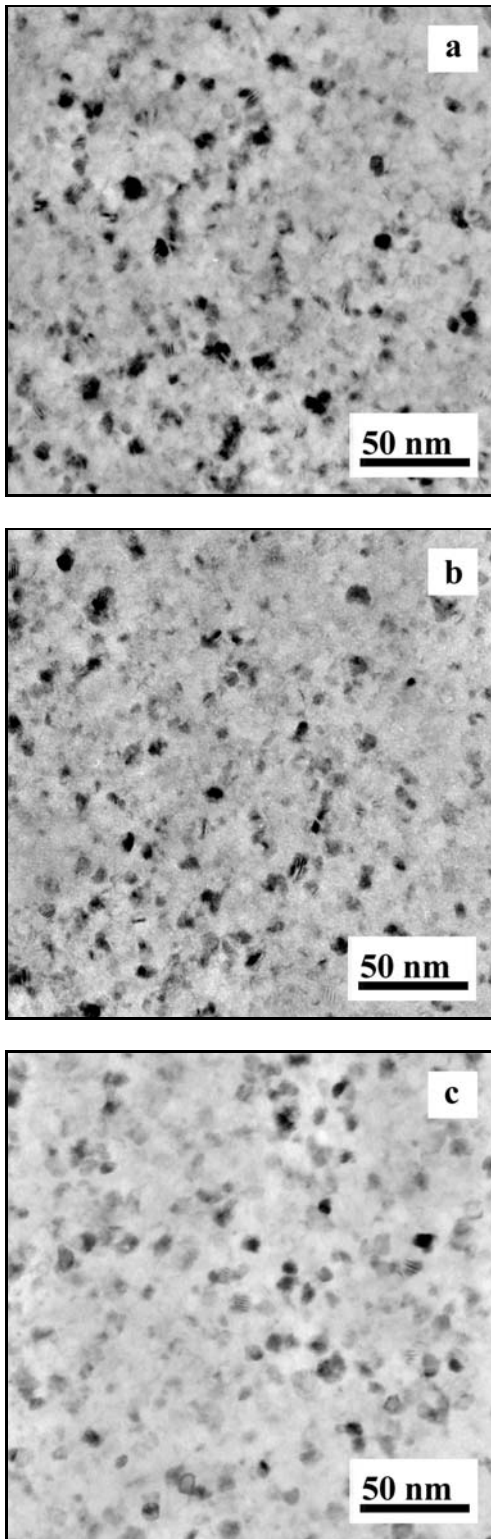


Fig. 9. TEM images of the $\text{Fe}_{80}\text{Zr}_7\text{Cu}_1\text{B}_{12}$ (a), $\text{Fe}_{80}\text{Zr}_4\text{Ti}_3\text{Cu}_1\text{B}_{12}$ (b) and $\text{Fe}_{80}\text{Ti}_7\text{Cu}_1\text{B}_{12}$ (c) alloys annealed at 650 °C, 650 °C and 620 °C, resp.

-quenched $\text{Fe}_{80}\text{Ti}_7\text{Cu}_1\text{B}_{12}$ is lower by almost 1 T than that of the $\text{Fe}_{80}\text{Zr}_7\text{Cu}_1\text{B}_{12}$. The highest hyper-

fine field in the as-quenched state was reached for $\text{Fe}_{80}\text{Zr}_4\text{Ti}_3\text{Cu}_1\text{B}_{12}$ but its increase as compared to the $\text{Fe}_{80}\text{Zr}_7\text{Cu}_1\text{B}_{12}$ is only minute.

Mössbauer spectra of annealed samples exhibited typical features of nanocrystalline alloys. They were decomposed into three components: amorphous, interfacial and crystalline. The crystalline phase formed was identified to be bcc-Fe. A close similarity (from the structural point of view) between crystalline phase and interfacial regions is demonstrated via dependences of B_{CR} and B_{IF} upon temperature of annealing which follow the same tendency. The IF spectral component represents Fe atoms located on the surface of the bcc-Fe nanograins (CR component). Deviations in the average hyperfine field of the amorphous residual phase (AM) with temperature of annealing are caused by changes in chemical short-range order due to progressing crystallization which modifies the composition because of significant depletion in Fe. The latter forms bcc crystalline grains in which tiny inclusions of Zr and/or Ti are also possible. Their amount should be only marginal because no appreciable changes in the hyperfine field values of the Mössbauer CR spectral components are observed. They cannot be, however, ruled out completely as the lattice parameters exhibit deviations from the values expected for pure bcc-Fe.

Acknowledgements

This work was supported by the grants VEGA 1/4011/07, 2/0157/08, APVV-0413-06, MSM6198959218 and CEX NANOSMART.

References

- [1] SUZUKI, K.—MAKINO, A.—INOUE, A.—MASUMOTO, T.: *J. Appl. Phys.*, **74**, 1993, p. 3316.
- [2] IDZIKOWSKI, B.—BASZYŃSKI, J.—ŠKORVÁNEK, I.—MÜLLER, K.-H.—ECKERT, D.: *J. Magn. Magn. Mater.*, **177–181**, 1998, p. 941.
- [3] MCHENRY, M.—WILLARD, M. A.—LAUGHLIN, D. E.: *Prog. Mater. Sci.*, **44**, 1999, p. 291.
- [4] HASEGAWA, R.: *J. Magn. Magn. Mater.*, **215–216**, 2000, p. 240.
- [5] MIGLIERINI, M.—VITTEK, R.—HASIAK, M.: *Mater. Sci. Eng. A*, **449–451**, 2007, p. 419.
- [6] WÜRSCHUM, R.: *Nanostruct. Mater.*, **6**, 1995, p. 93.
- [7] ČERMÁK, J.—STLOUKAL, I.: *Kovove Mater.*, **43**, 2005, p. 338.
- [8] ČERMÁK, J.—STLOUKAL, I.: *Kovove Mater.*, **44**, 2006, p. 307.
- [9] MIGLIERINI, M.—GRENECHE, J.-M.: *J. Phys.: Condens. Matter*, **15**, 2003, p. 5637.
- [10] HASIAK, M.—MIGLIERINI, M.—KALETA, J.—ZBROSZCZYK, J.—ZSCHESCH, E.: *J. Magn. Magn. Mat.*, **320**, 2008, p. 783.
- [11] HASIAK, M.—MIGLIERINI, M.—KALETA, J.—ZBROSZCZYK, J.—FUKANAGA, H.: *Mater. Sci. Poland*, **26**, 2008, p. 167.

- [12] ŽÁK, T.—JIRÁSKOVÁ, Y.: *Surf. Interf. Anal.*, **38**, 2006, p. 710.
- [13] MIGLIERINI, M.—GRENECHE, J. M.: *J. Phys.: Condens. Matter*, **9**, 1997, p. 2303.
- [14] ROUPCOVÁ, P.—SCHNEEWEISS, O.—BEZDIČKA, P.—PETROVIČ, P.: *Kovove Mater.*, **44**, 2006, p. 127.
- [15] RAFAJA, D.—KLEMM, V.—SCHREIBER, G.—KNAPP, M.—KUŽEL, R.: *J. Appl. Cryst.*, **37**, 2004, p. 613.
- [16] RAFAJA, D.: *Materials Structure*, **14**, 2007, p. 67.